Z. Phys. D 40, 229–235 (1997)

ZEITSCHRIFT
FÜR PHYSIK D

Comparison of reaction pathways calculated by different algorithms for disilane and water trimer

T. R. Walsh, D. J. Wales

University Chemical Laboratories, Lensfield Road, Cambridge CB2 1EW, UK

Received: 5 July 1996 / Final version: 26 September 1996

Abstract. There still exists some confusion in the literature concerning the definition of a minimum energy pathway and the coordinate system in which it is calculated. Here we compare steepest-descent and eigenvector-following pathways, both with and without a mass-weighted metric. The systems studied are disilane and the water trimer, and we employ various basis sets at the SCF level of theory. We find that paths calculated using eigenvector-following and steepest-descent are practically the same, at least in terms of the reaction mechanism. We find that for the mass-weighted metric the pathways are similar, although in principle they do not have to be identical. Finally, we verify that the geometrical symmetry selection rules hold for a pathway mediated by a recently discovered transition state of the disilane system.

PACS: 31.10.+z; 31.20.Ej; 36.40.+d

1 Introduction

Some confusion still seems to surround the issue of 'minimum energy' paths (MEP's) for chemical reactions, particularly their invariance in different coordinate systems, and whether pathways calculated by eigenvector-following [1-3] are generally close to steepest-descent paths. It is a misconception that an MEP, or strictly speaking, a steepest-descent path, is dependent on choice of coordinates [4]. There also exists the misconception that steepest-descent paths must be calculated in 'mass-weighted' coordinates [5], that is, using Fukui's 'kinetic metric' [6]. Quapp and Heidrich first advanced arguments to challenge this idea in 1984 [7], and followed this work with a similar paper some years later, which focussed on the mass-weighting of coordinates [8]. More recently, Bannerjee and Adams [9] have proved the coordinate invariance of steepest-descent paths using tensor algebra. These authors also discuss coordinate transformations, particularly to the Hessian eigenvalue representation. It has previously been suggested that non-unitary transformations to internal coordinates do not preserve the Hessian eigenvalues and eigenvectors [10]. However, this problem can be dealt with by defining the gradient and Hessian so that they transform like first and second rank covariant tensors, respectively. It follows that if care is taken to include the metric tensor of the coordinate system, then any path which makes use of the gradient and Hessian in this way is invariant to changes in the coordinate system.

The paths traced out by eigenvector-following minimisations are not necessarily identical to steepest-descent paths on the potential energy surface (PES). This is because the eigenvector-following step is not strictly anti-parallel to the negative gradient vector. Furthermore, Sun et al. [11] have shown that the paths produced by such quasi-Newton methods may not compare favourably with the true steepest-descent path. All quasi-Newton methods generally choose the local search direction as the line connecting the current point with the critical point in the region of a local quadratic approximation. However, the surface may not be quadratic at all in the region between the current point and the actual minimum, and so the direction from the critical point in the local quadratic approximation may not be aligned with the real minimum.

Sun et al. showed that paths from quasi-Newton methods may be quite different from and even orthogonal to the true steepest-descent path. They tested their steepest-descent algorithm against a quasi-Newton minimization (the UMING code [12]) on the Müller-Brown model surface for sixteen different starting points and for step sizes of length 0.1, 0.2, and 0.3 Å. Not only should the calculated path follow the true path, but it should also lead to the same minimum consistently for different step sizes. The authors conclude that the quasi-Newton paths are very unreliable, and may not even converge to the correct minimum. However, the quasi-Newton paths actually appear to follow the true paths quite satisfactorily when the initial point corresponds to a saddle point. For starting points in all other areas of the sample surface, the correspondence between the quasi-Newton and steepest-descent paths certainly looks poorer. However, the quasi-Newton paths of interest in this study are those which start from a saddle of index one, i.e. a stationary point with one negative Hessian eigenvalue. Regardless of the fact that the sample surface is a two-dimensional one, and pathological at that, the findings of Sun et al. for quasi-Newton paths starting from transition states are reassuring.

Wales [13] recalculated the sixteen paths using an eigenvector-following algorithm [14], and compared them with the corresponding true steepest descent paths on the Müller-Brown model surface. While the sixteen starting points are probably not exactly the same as those used by Sun et al., they should be close enough to get an idea of the general quality of the eigenvector-following paths. In agreement with Sun et al., the performance for the eigenvector-following paths which start from points which are not saddles is quite poor, even for a step size of 0.025 Å. The eigenvector-following paths starting from the two saddle points actually follow the true steepest-descent paths quite faithfully for a step size up to 0.2 Å. As a further example, Wales calculated steepest-descent and eigenvector-following paths for the five most pathological pathways calculated for a 55-atom cluster modelled using a Lennard-Jones potential. A visual comparison between the different paths was achieved by determining which two coordinates change the most along the pathway, and plotting them against each other. The five test paths were all initiated from true transition states (stationary points of Hessian index one [15]) following small displacements parallel and anti-parallel to the Hessian eigenvector corresponding to the single negative Hessian eigenvalue. For a maximum step size of 0.17Å, the steepest-descent and eigenvector-following paths appeared to be almost identical for all of the five paths. The eigenvector-following algorithm used in the present work employs the same form for the steps combined with a trust-radius for each degree of freedom, as described elsewhere [16].

It remains to examine the behaviour of steepest-descent and eigenvector-following paths on an ab initio PES. We will confine ourselves to paths linking transition states to minima, since these are by far the most chemically important. We expect, in view of the results above, that the eigenvector-following and steepest-descent paths should not be very different for such cases.

We have considered pathways for two systems, disilane, Si_2H_6, and the water trimer, calculated both with and without mass-weighting of the Cartesian coordinates, using both eigenvector-following and steepest-descent techniques. We expect paths calculated with and without the 'kinetic metric' [9] will be different, but not substantially so.

2 Computational details

All of the paths were calculated for ab initio surfaces at the SCF level. We employed a standard 6-31G** [17] basis for both disilane and water trimer and also used a standard 4-31G [18] basis for the water trimer only. Analytic first and second derivatives were calculated with the CADPAC [19] package. The minimization, transition-state searching and reaction path calculations were all performed using our OPTIM program.

Mass weighting was introduced into the steepest-descent and eigenvector-following calculations by transforming the $3N$ Cartesian coordinates $\{X^1, X^2, ..., X^{3N}\}$ according to

$$Q^i = \sqrt{m_i} X^i, \tag{1}$$

where m_i is the atomic mass of atom i. This transformation alters the metric tensor, changing it from **I** (the identity) to the $3N \times 3N$ matrix **M** with atomic masses on the diagonal. The transformed gradient and Hessian are then:

$$G'_i = \frac{G_i}{\sqrt{m_i}} = \frac{1}{\sqrt{m_i}} \frac{\partial E}{\partial X^i},$$

$$H'_{i,j} = \frac{H_{i,j}}{\sqrt{m_i m_j}} = \frac{1}{\sqrt{m_i m_j}} \frac{\partial^2 E}{\partial X^i \partial X^j}. \tag{2}$$

The projection operator suggested by Page and McIver [20] was used to project out overall translation and rotation following Baker and Hehre [21]. For the steepest-descent calculations we used Pechukas' path parameterisation [22]; details of the eigenvector-following calculations have been described elsewhere [16]. In each case the pathways were initiated following infinitesimal displacements parallel and anti-parallel to the transition vector, as described above. It is difficult to visualise paths in many-dimensional space in order to compare them. After comparing animations of the pathways by eye, we considered the energy as a function of the integrated path length S defined as

$$S = \sum \Big[\sum_i (\Delta X^i)^2 \Big]^{\frac{1}{2}}, \tag{3}$$

where the outer sum is over the steepest-descent and eigenvector-following steps, as appropriate. If the paths appear different at this level, there is no need to devise more complicated methods of comparison. If they look the same then for the present purposes we consider the agreement satisfactory.

The problem of an indefinite path length for dissociative reactions was dealt with by implementing an energy cutoff criterion. This cutoff ensures that the path lengths calculated for different methods are directly comparable.

3 Results for disilane

Disilane can follow a number of dissociation channels, the most likely being the elimination of molecular hydrogen or silane. Three such pathways have been characterized theoretically. Gordon et al. [23] examined two competitive channels which involve molecular hydrogen elimination, and in particular the reaction which produces disilene and molecular hydrogen. Previous theoretical and experimental studies have characterised the disilane molecule [24, 25]. Theoretical studies on the disilene molecule have found the structure to be slightly bent, in agreement with experiment [25]. Minima corresponding to the silane and the disilene molecule have also been found [26] along with a transition state of C_1 symmetry between the silane minimum and the disilane/H_2 complex. Gordon et al. also calculated Fukui's intrinsic reaction coordinate [6] at the SCF/3-21G* level.

Recently, this system was revisited as a test case for a new transition state search algorithm [27] which found one new transition state with C_2 symmetry corresponding to the same decomposition at the SCF/6-31G** level. The barrier for the pathway passing through this new transition state is reported to be 8.4 kJ/mol higher than that for the C_1 transition state. The authors report that the product of the decomposition via the C_2 transition state is a complex of the Si_2H_4

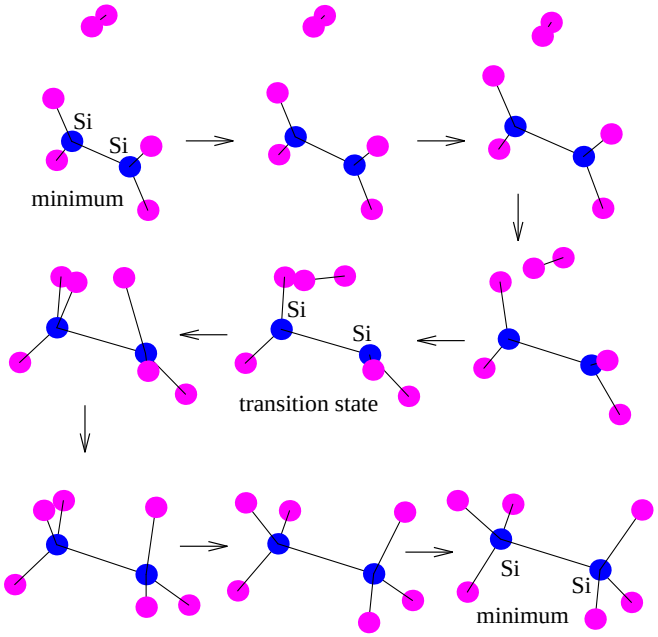

Fig. 1. Plot of geometry changes along path2 for Si_2H_6 calculated using eigenvector-following at the SCF/6-31G** level

and H_2 molecules with C_1 symmetry, and note that this result appears to be in violation of the symmetry selection rules of Stanton and McIver [10]. Pechukas [22] provides a particularly clear account of the rules for conservation governing nuclear symmetry along a steepest-descent path, and further deduces restrictions on the possible symmetries of transition states. Non-symmetric bimolecular decomposition reactions are also given some attention in the latter paper, where Pechukas arrives at the following conclusions:

(1) A transition state leading to a bimolecular product and/or reactant may have at most one axis of rotation, and any plane of reflection must contain the centres of mass of the separated molecules. It follows that the transition state point group will be of the form C_n or C_{nv}.

(2) Each of the separated molecules in this type of reaction must have the above group as a subgroup of their own point group.

(3) Nuclei which are symmetry related in the transition state must be related in the same manner in both the reactant and product molecules.

The stationary points corresponding to the disilane minimum and the C_1 transition state structure of Gordon et al. [23], as well as the recently discovered C_2 transition state structure, were all reoptimised starting from the geometries quoted by Ionova and Carter [27], for both STO-3G (with a set of d functions on the Si atoms) and 6-31G** basis sets. The C_2 transition state and the disilane minimum were also optimized at the DZP level. The point groups, the number of negative Hessian eigenvalues and the calculated energies for each basis are given in Table 1.

The C_1 and C_2 transition states will here be denoted as ts1 and ts2 respectively, with associated pathways path1 and path2. Both paths were calculated with the STO-3G and 6-31G** basis sets at the SCF level, both with and without mass-weighting and using both steepest-descent and eigenvector-following routines.

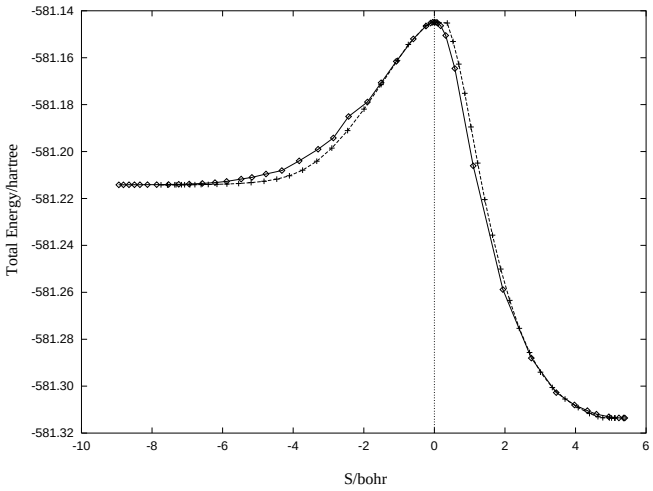

Fig. 2. Plot of energy against path length for path2. The path marked by *diamonds* was calculated by eigenvector-following and the path marked by *crosses* by steepest-descent, at the SCF/6-31G** level

Table 1. Total energies ($E/$ hartrees), number of imaginary normal mode frequencies (λ) and point groups calculated for the min, ts1 and ts2 structures of Si_2H_6

		DZP/SCF	6-31G*/SCF	STO-3G/SCF
min	E	-581.31659	-581.31357	-574.84172
	λ	0	0	0
	Point Group	D_{3d}	D_{3d}	D_{3d}
ts1	E		-581.14483	-574.58867
	λ		1	1
	Point Group		C_1	C_1
ts2	E	-581.14794	-581.14801	-574.57983
	λ	1	1	1
	Point Group	C_2	C_2	C_2

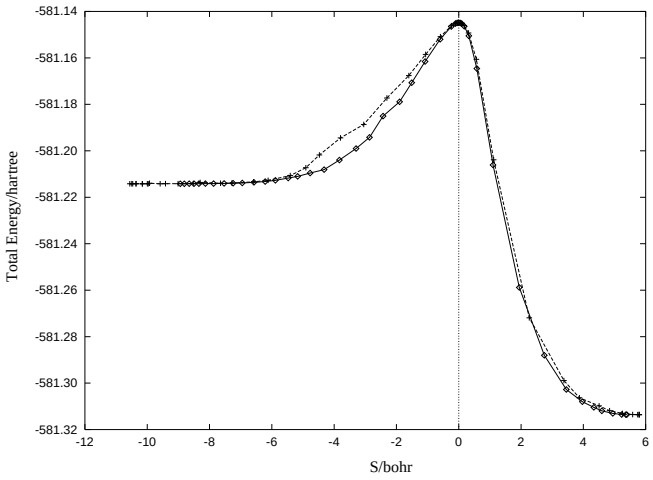

Fig. 3. Plot of energy against path length for path2. The path marked by *diamonds* was calculated without mass-weighting, and the path marked with *crosses* with mass-weighting. These paths were calculated with the eigenvector-following method at the SCF/6-31G** level

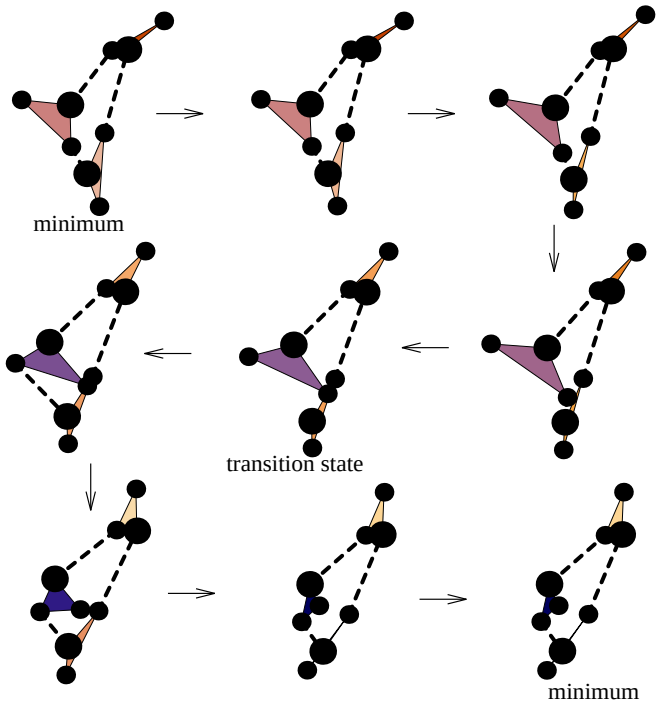

Fig. 4. Plot of geometry changes for $(H_2O)_3$ along the eigenvector-following path calculated at the SCF/4-31G level

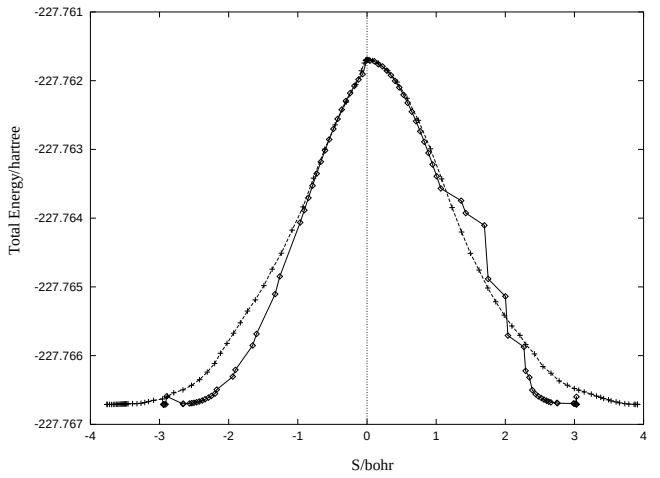

Fig. 5. Plot of energy against path length for $(H_2O)_3$. The path marked by *diamonds* was calculated by steepest-descent, and the path marked by *crosses* by eigenvector-following, both at the SCF/4-31G level

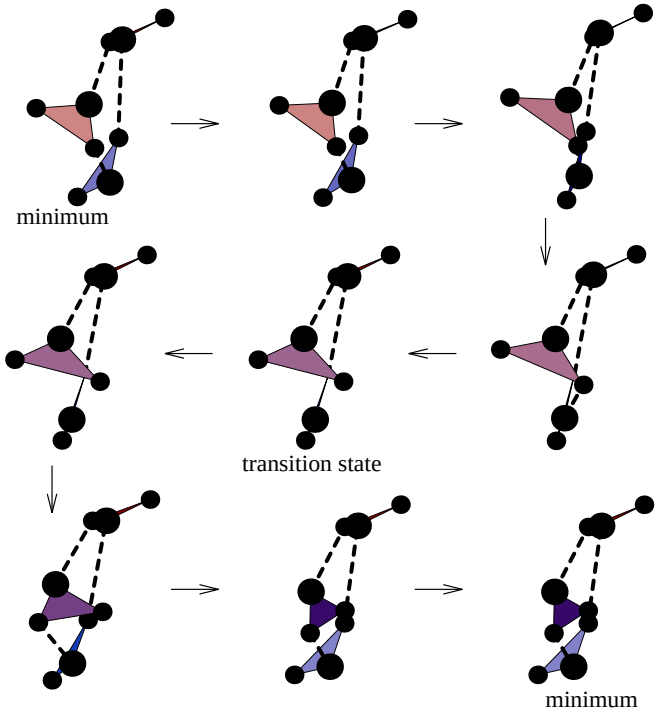

Fig. 6. Plot of geometry changes for $(H_2O)_3$ along the eigenvector-following path at the SCF/6-31G** level

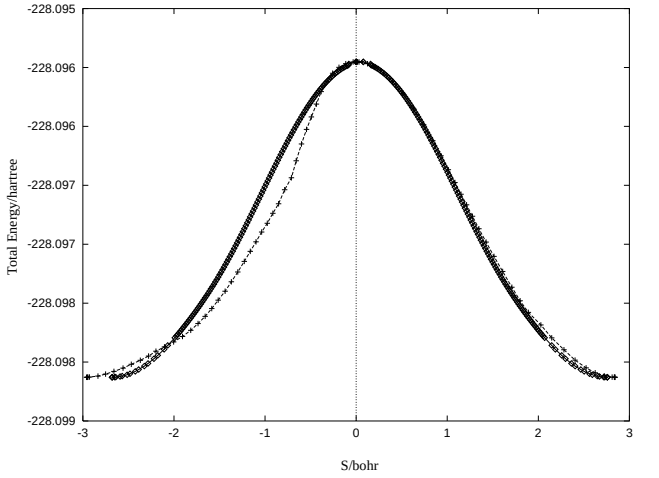

Fig. 7. Plot of energy against path length for $(H_2O)_3$. The path marked by *diamonds* was calculated by steepest-descent, and the path marked by *crosses* by eigenvector-following, at the SCF/6-31G** level

4 Comparison of eigenvector-following and steepest-descent pathways

Figure 1 shows the change in geometry along path2 at the SCF/6-31G** level calculated with eigenvector-following in terms of nine 'frames', four of which are from one side of the path, four from the other side, and with the transition state in the centre.

The pathways calculated here for path2 are visually indistinguishable for all the methods we applied. The same is true for path1. Having established that the different methods of calculating the path result in the same reaction mechanism we proceed to the next level of comparison, i.e. energy as a function of path length, S.

Comparisons made between steepest-descent and eigenvector-following versions of path2 at the SCF/6-31G** level are shown in Fig. 2. While the paths are not identical, they certainly appear very similar. From the analysis of Sun et al. [11] one would expect to observe a maximum discrepancy in the regions between the transition state and the minimum where the surface is not necessarily dominated by quadratic terms in the energy expansion. This does indeed appear to be the case here, especially for the dissociative path.

On the basis of these admittedly limited comparisons, we conclude that the paths obtained from steepest-descent and eigenvector-following for this system show no great discrepancies. Hence we can use whichever is most convenient or efficient.

5 Comparison of paths calculated with the kinetic metric

In the Introduction, we noted that some confusion still exists in the literature concerning the validity of non-mass-weighted paths when trying to calculate a reaction mechanism. When full covariant derivatives are considered, paths calculated in different coordinate systems are the same [9]. Here we consider paths calculated in mass-weighted coordinates when the incomplete partial energy derivatives of the energy are considered. This is equivalent to employing a fictitious 'kinetic metric' as explained by Bannerjee and Adams [9]. Hereafter we will simply refer to such coordinates as 'mass-weighted' for convenience.

The same methods are used to compare path1 and path2 as in Sect. 4, using both mass-weighted (the fictitious 'kinetic metric') and non-mass-weighted Cartesian coordinates. We first confirmed that the paths terminate at the same minima, and follow the same reaction mechanisms as before. We found that the reaction mechanisms for path1 and path2 are essentially unchanged when the 'kinetic metric' is employed.

We again followed this initial check with a comparison of the energy as a function of path length. The paths in this case can be compared for both the steepest-descent and eigenvector-following frameworks. Figure 3 shows the results for path2 using the eigenvector-following method. It shows that non-mass-weighted and mass-weighted paths lie very close to each other, particularly for the branch leading to the disilane minimum. The discrepancies observed for the dissociative branch are larger—this can probably be attributed to the fact that the Si_2H_4/H_2 complex is reasonably floppy. Since steps with the kinetic metric are not the same as those without, it seems reasonable that the difference between paths will become more pronounced if the PES is flat.

Path1 shows similar behaviour to path2. Overall, the non-mass-weighted paths and mass-weighted paths calculated with the eigenvector-following method are very similar at this level of comparison.

The same comparisons may be made for paths calculated by steepest-descent; our conclusions are the same as for eigenvector-following above. Paths 1 and 2 determined at the STO-3G level also follow this pattern.

Ionova and Carter [28] have previously tried to explain why the C_2 transition state does not violate the geometrical symmetry selection rules in terms of the dissociative nature of the path. However, a C_2 transition state is in fact allowed for this bimolecular reaction. It can be seen in Fig. 1, for example, that not only is the C_2 axis preserved throughout the entire reaction, but that the three individual molecules, disilane, disilene and hydrogen, all possess the C_2 symmetry element. It is also clear that the same nuclei are symmetry related to each other in each of these individual molecules. Hence, the C_2 transition state is not forbidden for this reaction.

6 Results for the water trimer

It is currently accepted that the global minimum of the water trimer cluster is a cyclic structure [28, 29]. The PES of the water trimer system has been shown to exhibit highly anisotropic behaviour in the region of the two low energy degenerate rearrangements. Using both *ab initio* and empirical potentials, Wales [30] determined reaction mechanisms and predicted tunnelling splitting patterns for this system. It was shown that when zero-point corrections are included, the barrier for the lowest energy mechanism (the 'flip') is virtually zero [31]. In the 'flip' mechanism, one of the free hydrogens migrates from one side of the plane defined by the oxygen atoms to the other side. In subsequent work we have concentrated on the second lowest energy mechanism, which we named 'bifurcation tunnelling' [32]. In this process

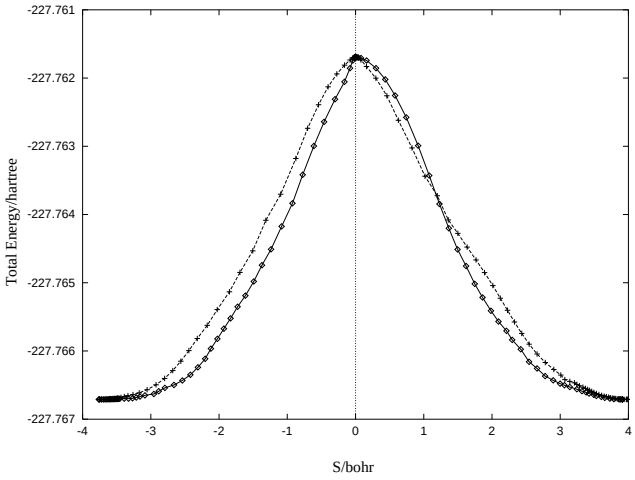

Fig. 8. Plot of energy against path length for $(H_2O)_3$. The path marked by *diamonds* was calculated by eigenvector-following without mass-weighting, and the path marked by *crosses* with mass-weighting, at the SCF/4-31G level

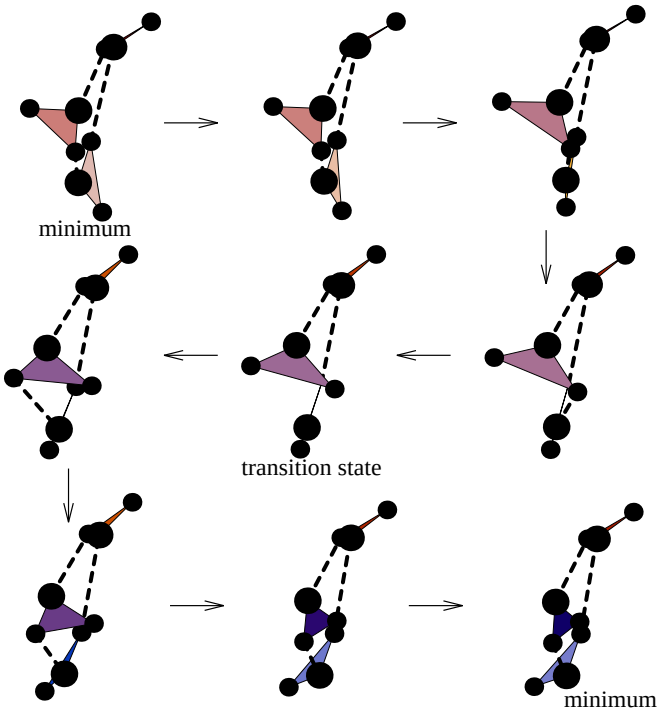

Fig. 9. Plot of geometry changes for $(H_2O)_3$ along the eigenvector-following path with mass-weighting at the SCF/6-31G** level

one molecule adopts a bifurcated hydrogen bonding pattern in the transition state, and this motion is accompanied by zero, one or two flips for the remaining two monomers, depending on the level of calculation [32]. The number of flips showed no convergence for the most accurate methods we could apply.

To distinguish each type of mechanism, we refer to the arrangement of the free hydrogens above or below the plane of the ring in the two minima. The two monomers which have terminal hydrogens on the same side of the O-O-O plane are referred to as 'majority' monomers, while the remaining water molecule is labelled the 'minority'. The monomer which undergoes the bifurcation can be either majority- or minority-type. If it is a majority monomer then there are two to choose from, and these may be identified in relation to the minority molecule. We call the majority monomer which acts as a hydrogen-bond donor to the minority monomer the 'majority donor' and the other one is then the 'majority acceptor'. If the minority monomer undergoes bifurcation then the same donor/acceptor relationships may be used to identify associated flips on the majority monomers. A more detailed analysis is given in reference [32].

We calculated the bifurcation pathway by eigenvector-following and steepest-descent with both mass-weighted and non-mass-weighted coordinates at the SCF/4-31G and SCF/6-31G** levels.

7 Comparison of eigenvector-following and steepest-descent pathways

For the 4-31G basis, the eigenvector-following pathway was found to be of the 'minority plus double flip' type. The pathway was also determined using steepest-descent and found to be essentially the same; the eigenvector-following path is shown in Fig. 4. Plots of the energy against path length are given in Fig. 5.

Figure 6 shows path2 calculated by eigenvector-following with the 6-31G** basis. Again there was no discernible difference in the reaction mechanism when compared to steepest-descent and in both cases the pathway was found to be of the 'majority donor plus no flip' type. Plots of energy versus path length are also very similar (Fig. 7).

As for disilane, we found little difference between eigenvector-following and steepest-descent pathways at the present level of comparison.

8 Comparison of paths calculated with the kinetic metric

Steepest-descent and eigenvector-following pathways calculated at the SCF/4-31G level with the kinetic metric were observed to retain the same 'minority plus double flip' mechanism as shown in Fig. 4. The energy as a function of the path length for eigenvector-following both with and without mass-weighting is shown in Fig. 8. The paths show differences which are slightly larger than for the disilane system. As was remarked before, paths with and without mass-weighting are not expected to be identical for floppy systems, as is the case here.

The 'mass-weighted' paths calculated with the 6-31G** basis were found to be qualitatively different in terms of the reaction mechanism. With the mass-weighted metric the steepest-descent and eigenvector-following pathways are both of the 'majority donor plus single flip' type, as shown in Fig. 9, in contrast to the 'majority donor plus no flip' mechanism described above. Since the mechanisms are different we omit plots of energy against path length.

The above behaviour is not surprising, considering that the PES for this system is very flat and anisotropic, and that the number of flips accompanying the 'bifurcation' mechanism is highly sensitive to the level of theory [32]. In this case we also considered the effect of changing the size of the initial displacement from the transition state. However, no dependence on this parameter was found over a wide range of values [32].

9 Conclusions

In this paper we have compared reaction pathways in disilane and the water trimer calculated by eigenvector-following and steepest-descent techniques using both mass-weighted and non-mass-weighted coordinates. In every case the eigenvector-following and steepest-descent paths are visually indistinguishable, and the energy as a function of path length is also very similar. We conclude that eigenvector-following pathways should generally give a satisfactory account of reaction mechanisms, notwithstanding the fact that paths initiated away from transition states can differ significantly from steepest-descent paths [11]. For disilane the paths calculated in mass-weighted and non-mass-weighted coordinates are essentially the same. However, for water trimer we found one qualitative difference in mechanism for the bifurcation tunnelling pathway calculated at the SCF/6-31G** level. This reflects the extreme sensitivity of the number of flips associated with the bifurcation mechanism to details of the calculation, and the fact that the pathways calculated with different metrics need not be the same. Consideration of the zero-point energy in coordinates orthogonal to the minimum energy path may be of use in elucidating further differences between paths defined with different metrics.

In the examples we have chosen practically all of the motion is associated with hydrogen atoms. If there were significant heavy atom motion too then we might expect more differences between the mass-weighted and non-mass-weighted paths. Nevertheless, the pathological example of the water trimer serves as a warning that different metrics can lead to somewhat different realisations of the mechanism, especially for very flat potential energy surfaces.

T.R.W and D.J.W thank the Cambridge Commonwealth Trust and the Royal Society for financial support, respectively.

References

1. Cerjan, C. J., Miller, W. H.: J. Chem. Phys. **75**, 2800 (1981)
2. Simons, J., Jørgenson, P., Taylor, H., Ozment, J.: J. Phys. Chem. **87**, 2745 (1983); O'Neal, D., Taylor, H., Simons, J.: J. Phys. Chem. **88**, 1510 (1984) Banerjee, A., Adams, N., Simons, J., Shepard, R.: J.

Phys. Chem. **89**, 52 (1985); Baker, J.: J. Comput. Chem. **7**, 385 (1986); **8**, 563 (1987)
3. Pancíř, J.: Collect. Czech. Chem. Commun. **40**, 1112 (1974)
4. Schlegel, H. B.: J. Chem. Soc., Faraday Trans. **90**, 1 (1994)
5. Page, M., McIver Jr., J. W.: J. Chem. Phys. **88**, 922 (1988)
6. Fukui, K.: J. Phys. Chem. **74**, 4161 (1970)
7. Quapp, W., Heidrich, D.: Theo. Chem. Acta (Berl) **66**, 245 (1984)
8. Quapp, W., Daschel, H., Heidrich, D.: J. Mol. Struct. (Theochem) **205**, 245 (1990)
9. Bannerjee, A., Adams, N. P.: Int. J. Quantum Chem. **43**, 855 (1992)
10. Stanton, R. E., McIver Jr., J. W.:J. Amer. Chem. Soc. **97**, 3632 (1975)
11. Sun, J. -Q., Ruedenberg, K., Aitchy, G. J.: J. Chem. Phys. **99**, 5276 (1993)
12. IMSL MATH/LIBRARY, IMSL Problem Solving Software Systems, Houston, TX, 1989, Sec. 8.1.2. Program UMING: quasi-Newton method using analytic gradients
13. Wales, D. J.: J. Chem. Phys. **101**, 3750 (1994)
14. Wales, D. J.: J. Chem. Soc., Faraday Trans. **86**, 3505 (1990)
15. Murrell, J. N., Laidler, K. J.: Trans. Faraday Soc. **63**, 371 (1968)
16. Wales, D. J., Walsh, T. R.: J. Chem. Phys. **105**, 6957 (1996)
17. Hehre, W. J., Ditchfield, S. S., Pople, J. A.; J. Chem. Phys. **56**, 2257 (1972)
18. Francl, M. M., Pietro, W. J., Hehre, W. J., Binkley, J. S., Gordon, M. S., DeFrees, D. J., Pople, J. A.: J. Chem. Phys. **72**, 3654 (1982)
19. Amos, R. D., Rice, J. E.: CADPAC: the Cambridge Analytic Derivatives Package, Issue 4.0; Cambridge University: Cambridge, U.K., 1987
20. Page, M., McIver Jr, J. W.: J. Chem. Phys. **88**, 922 (1988)
21. Baker, J., Hehre, W. H.: J. Comp. Chem. **12**, 606 (1991)
22. Pechukas, P.: J. Chem. Phys. **64**, 1516 (1976)
23. Gordon, M. S., Truong T. N., Bonderson, E. K.: J. Amer. Chem. Soc. **108**, 1421 (1986)
24. Cowley, A. H.: Polyhedron **3**, 389 (1984)
25. West, R., Fink, M. J., Michl, J.: Science **214**, 1344 (1981)
26. Snyder, L. C., Wasserman, Z.: J. Amer. Chem. Soc. **101**, 5222 (1979)
27. Ionova, I. V., Carter, E. A.: J. Chem. Phys. **98**, 6377 (1993)
28. Xantheas, S. S., Dunning Jr., T. H.:J. Chem. Phys. **98**, 10 (1993)
29. Pugliano, N., Saykally, R. J.: Science **257**, 1937 (1992)
30. Wales, D. J.: J. Amer. Chem. Soc. **115**, 11180 (1993)
31. Fowler, J. E., Schaefer, H. F.: J. Amer. Chem. Soc. **117**, 446 (1995)
32. Walsh, T. R., Wales, D. J.: J. Chem. Soc., Faraday Trans. **92**, 2505 (1996)

This article was processed by the author using the LaTeX style file *pljour2* from Springer-Verlag.